Geometric and metabolic constraints on bone vascular supply in diapsids

Jorge Cubo, Jéromine Baudin, Lucas J. Legendre, Alexandra Quilhac, Vivian de Buffrénil

Geometric and metabolic constraints on bone vascular supply in diapsids

JORGE CUBO[1, 2, *], JEROMINE BAUDIN[1, 2], LUCAS LEGENDRE[1, 2], ALEXANDRA QUILHAC[1, 2] and VIVIAN DE BUFFRÉNIL[3]

[1] *Sorbonne Universités, UPMC Univ Paris 06, UMR 7193, Institut des Sciences de la Terre Paris (iSTeP), F-75005, Paris, France.*

[2] *CNRS, UMR 7193, Institut des Sciences de la Terre Paris (iSTeP), F-75005, Paris, France.*

[3] *Sorbonne Universités, MNHN Muséum National d'Histoire Naturelle, UMR 7207, Centre de Recherche sur la Paléobiodiversité et les Paléoenvironnements (CR2P), F-75005, Paris, France.*

[*]Corresponding author: UPMC, Université Pierre & Marie Curie, 4 place Jussieu, BC 19, F-75005, Paris, France. E-mail: jorge.cubo_garcia@upmc.fr

RUNNING TITLE: Bone vascular supply in diapsids

ABSTRACT

Periosteal, endosteal, and intracortical blood vessels bring oxygen and nutrients to and evacuate the metabolic byproducts from osteocytes. This vascular network is in communication with bone cells through a network of canaliculi containing osteocyte cytoplasmic processes. The geometric and physiologic contraints involved in the relationships between osteocytes (including canaliculi) and blood vessels in bones remain poorly documented in a comparative point of view. First we test the hypothesis (1) that osteocytes in endotherms may have higher energetic expenditure and may produce more metabolic byproducts than in ectotherms. For this, we test and find evidence for the prediction derived from this hypothesis that the maximum absolute thickness of avascular bone tissue is significantly higher in lepidosaurs than in birds. We also test two alternative hypotheses explaining the variation of bone vascular density in diapsids: (2a) As body mass increases, the relative effectiveness of vascular supply of the periosteum decreases because its surface increases proportionally to the second power of bone length, whereas bone mass to be supplied increases proportionally to the third power. Accordingly, we predict and find evidence that bone vascular density is directly related to bone size in both lepidosaurs and birds. The alternative hypothesis (2b) suggesting that bone vascular density, like mass-specific resting metabolic rate, may decrease as body mass increases has been refuted by these last results. Knowledge of the cytologic relationship between osteocytes and blood vessels in diapsids is poor. Here we also present preliminary results of a comparative cytologic study on such relationship.

KEYWORDS**:** birds - bone vascularisation – lepidosaurs – metabolism - size

INTRODUCTION

Osteocytes obtain nutriments and oxygen and evacuate their metabolic byproducts through cytoplasmic expansions located inside canaliculi and linked to vascular networks (Mishra, 2009). These vascular networks are housed within bone cortices (Brookes, 1971; Francillon-Vieillot *et al.,* 1990) and in the inner (endosteal) and outer (periosteal) connective tissues associated with the bones (Simpson, 1985). The geometric constraints that control the structure of the vascular networks and their final relationships with local and systemic metabolic processes have been very poorly studied at a comparative level (Mishra, 2009). We analyze here the impact of the scaling of metabolic rate on two bone histological features: the thickness of peripheral layer of avascular bone tissue and the density of bone vascular supply. Previous studies have shown that femoral cortices of small adult lepidosaurs and birds are avascular or almost avascular (Cubo *et al.*, 2005; Buffrénil *et al.,* 2008), so that osteocytes perform metabolic exchanges exclusively with the inner and outer connective tissues. In birds, the relative thickness of the outer layer of avascular bone tissue scales to bone size with negative allometry (Ponton *et al.,* 2004). The maximum thickness of avascular bone in lepidosaurs and birds could be explained by a main hypothesis: (1) Osteocytes in endotherms have higher energetic expenditure and produce more metabolic byproducts than in ectotherms, which suggests that when bone cortical vascularization is absent endotherms need to have thinner layers of avascular bone, if transport of metabolites via canaliculi is under similar constraints in the different taxa. We thus expect significantly higher thickness of avascular bone tissue in lepidosaurs than in birds. Moreover, we analyzed the scaling of bone vascular density in the bones that actually

display vascular canals. Two antagonist factors could possibly explain the variation of this feature: Considering that mass-specific resting metabolic rate (oxygen consumption, in ml/h, per body mass, grams) decreases as body mass increases, we expect that the metabolic demands of osteocytes do likewise, in which case bone vascular density should decrease as body mass increases (hypothesis 2b). Conversely, as bone size increases, the vascular supply of the periosteum decreases in relative effectiveness because its surface increases proportionally to the second power of bone length, whereas bone mass (to be supplied) increases proportionally to the third power. So we expect that bone vascular density increases as body mass increases to compensate the smaller relative effectiveness of vascular supply of the periosteum (hypothesis 2a). It is well documented that osteocytes communicate with each other through the lacunocanalicular system (Mishra, 2009), but knowledge on the cytologic relationship between osteocytes and blood vessels (intracortical, endosteal and periosteal) in diapsids is poor. Here we present also preliminary results of a comparative cytologic study on such relationship.

MATERIAL AND METHODS

The analysis of the effect of the scaling of metabolic rate on the histological features was performed using a sample of femora of 46 species of lepidosaurs and 30 species of birds. Only adult animals were used and all the sections were made in a transverse plane located at mid-diaphysis to work in a strict frame of homology (Legendre *et al.,* this issue). The thin sections belong to preexisting collections at the Pierre & Marie Curie University, Paris (sample of birds) and the Muséum National d'Histoire Naturelle of Paris (sample of lepidosaurs). We quantified a number of cross-

sectional geometric and histological features using ImageJ (Schneider, Rasband & Eliceiri, 2012): bone cross-sectional area (the area encircled by the periosteum, including the medullary cavity); bone cortical area : black plus grey in Fig. 1B : bone cross-sectional area (including vascular canals) minus medullary cavity area; bone vascular area (in black in Fig. 1B : the area occupied by vascular cavities); total number of vascular canals in a bone section; and the mean thickness of the outer layer of avascular bone tissue (in black in Fig. 1C) measured as the radius of a circle of area equal to bone cross sectional area minus the radius of a circle of area equal to the area encircled by the outermost vascular canals (i.e. the area containing all intracortical vascular canals). When vascular canals were absent, we measured the mean thickness of the whole cortex. Bone vascular density was computed as total number of vascular canals / bone cortical area. Moreover we analyzed bone vascular area / bone cortical area. In birds, when only a few (less than ten) blood vessels were present in a bone section, the bone was considered to be avascular because they probably were blood vessels running from the periosteum to the endosteum (nutrient canals), and so did not form a vascular network inside the bone cortex. All variables but the ratios were log transformed in order to spread the points more uniformly in the graphs to improve the interpretability. We analyzed only transverse sections but, considering that hydraulic resistance increases as the distance from osteocytes to blood vessel increases (Mishra, 2009), the key functional constraint is the distance from osteocytes to blood vessels (either intracortical or periosteal) in a given plane of section. In other words, a given osteocyte can in principle obtain nutrients from blood vessels located at different positions in the 3D space, but in a given plane of section, the distance from an osteocyte to a blood vessel must be lower than the threshold above which the transport of oxygen and nutriments is no longer possible because of hydraulic resistance. In this context,

because the critical biological constraint is the absolute distance from cells to blood vessels, we analyzed absolute (instead of relative to bone size) values of the thickness of the outer layer of avascular bone tissue and of the bone vascular density.

All statistical analyses were performed using the phylogenetic comparative method (*sensu* Harvey & Pagel, 1991). Phylogenetic relationships within the sample of birds used in this study (Fig. 2) were compiled from Barker, Barrowclough & Groth (2002) and Livezey & Zusi (2007). The phylogenetic tree of the sample of lepidosaurs used in this study (Fig. 3) was compiled from Ast (2001) and Conrad (2008). Branch lengths were estimated using Pyron (2010) for birds and Conrad (2008) for lepidosaurs. Regressions were performed using phylogenetic generalized least squares (Grafen, 1989). Pagel's lambda was compiled simultaneously with each regression via maximum-likelihood using the function pgls from R package 'caper' (Orme *et al.*, 2012), thus ensuring an accurate estimation of phylogenetic signal for each couple of variables (Revell, 2010): lambda = 0 means no phylogenetic signal; lambda = 1 means high phylogenetic signal (traits evolve following a Brownian motion model). The mean value for a given clade (i.e., lepidosaurs, birds) was obtained as the value for the root node computed using squared-change parsimony optimization (Maddison, 1991) in the PDAP module (Midford, Garland & Maddison, 2011) of Mesquite (Maddison & Maddison, 2011). The corresponding confidence intervals were also computed using the PDAP module of Mesquite.

The cytologic analysis of the relationship between osteocytes and blood vessels was performed using four subadult *Varanus exanthematicus* and four subadult *Anas platyrhynchos* (Fig. 4). They all originate from breeding. After euthanasia, femora were fixed

in a mixture containing 2.5% glutatraldehyde, 2 % paraformaldehyde in 0.1 M cacodylate buffer. The samples were demineralised using 5% EDTA added in the fixative. The demineralised samples were post fixed with 1% osmium tetroxide in the cacodylate buffer, dehydrated, and subsequently embedded in Epon. Semi-thin (1 μm) sections were stained with toluidine blue (pH 4) and examined using light microscopy. Thin (0.05 μm) sections were double-stained with uranyl acetate and lead citrate. The grids were viewed in a Zeiss Leo transmission electron microscope with an operating voltage of 80 kV.

RESULTS

Thickness of avascular bone tissue

In birds, the mean thickness of the outer layer of avascular bone tissue is 0.072 mm, with lower and upper 95% confidence intervals of, respectively, 0.034 and 0.109 mm. Variation ranges from 0.033 mm in *Podiceps cristatus* to 0.122 mm in *Dendrocopos major*. In birds this layer was always present. In some species, the entire cortex is avascular: *Emberiza citrinella, Erithacus rubecula, Sylvia atricapilla, Parus caeruleus, Apus apus, Troglodytes troglodytes* and *Parus major* (table 1).

In lepidosaurs, vascular canals, when present, appear throughout bone cortex, from depth to periphery, so no outer layer of avascular bone tissue was defined. Instead, we analyzed the thickness of the cortex in a subsample of lepidosaurs containing exclusively species with avascular femora (see table 2). We obtained a mean thickness of the cortex in lepidosaurs with avascular femora of 0.790 mm with lower and upper 95%

confidence intervals of, respectively, 0.381 and 1.199 mm. The range of variation is: 0.058 mm in *Coleonyx elegans* and 1.455 mm in *Amblyrhychus cristatus.*

We also regressed the log thickness of the outer layer of avascular bone tissue with log bone cross-sectional area in birds and did not find a significant relationship between these variables. The regression of log thickness of the outer layer of avascular bone tissue with log bone radius in birds is not significant either (Pagel's Lambda: 0.000; adjusted R^2: 0.04; *p*-value: 0.146; Fig. 5).

Bone vascular density

Bone vascular density (computed as number of vascular canals / bone cortical area) is positively related to log bone cross-sectional area in both lepidosaurs (Pagel's Lambda: 0.225; R^2: 0.112; *p*-value: 0.007) and birds (Pagel's Lambda: 1.000; R^2: 0.2629; *p*-value: 0.002). The ratio of bone vascular area / bone cortical area is also positively related to log bone cross-sectional area in in both lepidosaurs (Pagel's Lambda: 0.000; R^2: 0.1703; *p*-value: 0.001) and birds (Pagel's Lambda: 1.000; R^2: 0.2398; *p*-value: 0.003). Finally, bone vascular density is also related to log snout-vent maximal length in *Varanus* (Pagel's Lambda: 0.000; R^2: 0.2102; *p*-value: 0.024; Fig. 6). In *Varanus,* femora with a bone cross-sectional area of more than 8 mm^2 are vascularized. In the whole clade Lepidosauria, no femur smaller than 8 mm^2 is vascularized. However, many species with femora of bone cross-sectional area bigger than 8 mm^2 are avascular: *Uromastyx aegyptiacus* (10.7905 mm^2), *Heloderma horridum* (13.2185 mm^2), *Iguana iguana* (17.8433 mm^2), *Gallotia goliath* (18.3900 mm^2), *Ctenosaura pectinata* (23.0215 mm^2), and *Amblyrhynchus cristatus* (29.158 mm^2).

Cytologic analysis of the relationship between osteocytes and blood vessels

Anas platyrhynchos. The well-vascularized femoral periosteal bone tissue contains a rich osteocyte network (Fig. 4A, B). Osteocytes are numerous around vascular canals. Their canaliculi clearly point towards blood vessels (Fig. 4B). In the periosteum, some osteoblasts are in close contact with capillary blood vessels (Fig. 4A). TEM images confirm the presence of a tight relationship between osteocytes and blood vessels (Fig. 4E). These osteocytes show a prominent nucleus and endoplasmic reticulum in the cytosol (Fig. 4E). The contact is established between the plasmic membrane of the blood vessel endothelial cell and the plasmic membrane of the osteocyte processes. Multiple canalicular projections protrude from the osteocyte body in all directions.

Varanus exanthematicus. The bone cortex is typically composed of a parallel-fibered bone tissue and displays vascular canals that are evenly distributed. The osteocytes situated in the periphery of the bone cortex show long canaliculi directed towards the periosteum (Fig. 4C) whereas those situated around vascular canals in the cortex show canaliculi directed towards the wall of these blood vessels (Fig. 4D).

DISCUSSION

A series of hypotheses concerning the variation of bone vascularization in lepidosaurs and birds have been put forth in the introduction. We will successively discuss them. But before we will briefly discuss the results obtained in the cytologic analysis aimed at exploring the relationships between the osteocytes and the blood vessels.

Both animal models analyzed in this study (*Varanus exanthematicus* and *Anas platyrhynchos*) show a cortical network of canaliculi preferentially oriented towards the vascular canals (either intracortical or periosteal), which supply in nutrients and oxygen the bone cells (Currey, 2002 ; Bonewald, 2011; Kennedy & Schaffler, 2012). Considering that hydraulic resistance increases as distance from blood vessel increases, there may be a threshold above which the transport may not be possible. Mishra (2009) concluded that osteon diameter is determined by this threshold. Here we hypothesize that the thickness of avascular bone tissue depends on the metabolic demands of bone cells; therefore this thickness is likely to be higher in lepidosaurs than in birds. The 95% confidence intervals for birds and lepidosaurs do not overlap: the lower limit of the lizard confidence interval (0.381 mm) is more than three times higher than the upper limit of the bird confidence interval (0.109 mm). On the other hand, the mean avascular thickness is more than ten times thicker in lepidosaurs (0.790 mm) than in birds (0.072 mm). These results are strong evidence for hypothesis 1, according to which we expect a higher thickness of avascular bone tissue in lepidosaurs than in birds because osteocytes of the latter have higher energetic expenditure and produce more metabolic byproducts than those of the former. Our result of a maximum thickness of the avascular layer (i.e. the farthest distance of an osteocyte from a blood vessel located on the periosteum) of 0.122 mm in birds is astonishingly congruent with those published by Mishra (2009), according to which mammalian osteon diameter is of 0.250 mm (which would represent the double of the farthest distance -i.e. 0.125 mm- between an osteocyte and the osteonal vascular canal). Values obtained here for lepidosaurs with avascular bone are extremely high to transport nutrients and oxygen from connective tissues (endosteum and periosteum) to bone cells placed at the center of the cortex.

Mean thickness of the cortex in lepidosaurs with avascular femora is 0.790 mm and the higher value, found in in *Amblyrhychus cristatus,* is 1.455 mm (i.e. the distance from endosteal or the periosteal blood vessels and osteocytes located in the middle of the bone cortex is 0.727 mm). These values are higher than those previously cited by Mishra (2009) for the avascular bones of amphibians (distance between osteocytes and periosteal and endosteal blood vessels of 0.150 mm). This result is surprising because, for a body mass smaller than roughly 100 g, the standard metabolic rate (mL O_2 h^{-1}) of amphibians is smaller than that of "reptiles" (White, Phillips & Seymour, 2006).

Within birds, Ponton *et al.* (2004) showed that the ratio of the thickness of the outer layer of avascular bone tissue to bone cortical thickness scales with negative allometry relative to bone radius. This would mean that the bigger a bone, the thinner, relative to cortical thickness, its peripheral avascular layer. Here we have found that the absolute thickness of the outer layer of avascular bone tissue is independent from both bone cross sectional area and bone radius in birds. So we conclude that the negative allometry found by Ponton *et al.* (2004) reflects the fact that they analyzed relative values of outer avascular layer thickness. In other words, for a constant thickness of avascular bone, its relative thickness may decrease with increasing bone size. When analyzing absolute values (as has been done here), the thickness of the outer layer of avascular bone tissue is independent of bone size and so it may also be independent from body size.

Different factors have been evoked in the literature to explain the variation of bone vascularization in tetrapods. Our results allow a deeper knowledge on the determinism of bone vascularization in diapsids, as discussed below.

Phylogeny. Cubo *et al.* (2005) showed that the ratio bone vascular area / bone cortical area is explained by phyogeny at the nodes sauropsids, diapsids, archosaurs, lepidosaurs and birds, but not in testudines. Results obtained in this study for the sample of birds (Pagel's Lambda = 1.000 suggesting a high phylogenetic signal) agree with those of Cubo *et al.* (2005) and those by Legendre *et al.* (this issue). However, results obtained for lepidosaurs (Pagel's Lambda = 0.000 suggesting no phylogenetic signal) do not agree with those obtained by Cubo *et al* (2005), probably because these last authors used a smaller sample size. Buffrénil *et al* (2008) concluded that phylogeny does not explain the variation of the ratio of bone vascular area to bone cortical area in *Varanus.* Our results agree with their conclusion: we obtained a Pagel's lambda of 0.000 in the regression of bone vascular area / bone cortical area to snout-vent maximal length (both with and without log transformation) in *Varanus,* suggesting no phylogenetic signal in the variation of this feature.

Bone cross-sectional area and body size. Bone vascular density and the ratio of vascular canal area / bone cortical area are positively related to bone cross-sectional area in both lepidosaurs and birds. Results obtained here using PGLS regressions are congruent with those obtained by Cubo *et al* (2005) for sauropsids using phylogenetically independent contrasts. On the other hand, bone vascular density is related to snout-vent maximal length in *Varanus*. This last result is congruent with that obtained by Buffrénil *et al.* (2008) using a statistical methodology that did not include phylogeny. All these results may be interpreted as evidence for hypothesis 2a suggesting that bone vascular density increases as bone and body size increase to compensate the smaller relative effectiveness of vascular supply of the periosteum because periosteal

supply depends on periosteal area, and thus increase quadratically as compared to bone linear dimensions; conversely, bone volume or mass (to be supplied) increase faster, with the third power of bone linear dimensions. The endosteum is also a potential source of nutrients for bone cells. However, its relative contribution is smaller than that of the periosteum because the cement line separating endosteal from periosteal bone most likely disrupts the osteocyte network and prevents any communication between endosteal and periosteal canaliculi, as suggested by the fact that canaliculi are cut by, and do not have any communication through, the cement lines of secondary osteons (Kerschnitzki *et al.* 2011).

Metabolic rate. Mass-specific resting metabolic rate decreases as body mass increases (Schmidt-Nielsen, 1997; Hulbert *et al.* 2007). We expect that the metabolic demands of osteocytes do likewise, in which case bone vascular density and the ratio bone vascular area / bone cortical area may also decrease as body mass (tightly related to bone size) increases (our hypothesis 2b). We have found the opposite result, which refutes this hypothesis. However, a small effect of metabolic rate on bone vascularization may exist, as suggested by the following data: In *Varanus,* the threshold above which femora are vascularized is lower (bone cross-sectional area = 8 mm^2) than in other lepidosaurs, probably because the former have higher metabolic rates.

Bone growth rate. Buffrénil *et al* (2008) concluded that bone growth rate is the main proximal factor explaining the variation of bone vascularization in *Varanus*, in agreement wih Amprino's rule (Amprino, 1947). This explanation may be correct for the whole clade of diapsids when primary bone in the inner part of the cortex is analyzed. However, when the whole cortex is analyzed (as it is the case in the present study), we

must take into account the fact that bone growth rate decreases with age, so that some regions are formed at high rates (and show high vascular densities) whereas other, more peripheral (younger) regions show low or no vascularization of all. In birds, considering that the thickness of the outer avascular layer is independent from bone size and more or less constant, big species may retain at adulthood a bigger fraction of rapidly formed, densely vascularized, bone tissue than small species, which may retain exclusively the outer avascular layer.

In conclusion, bone vascular density, bone growth rate, bone cross-sectional area and mass-specific metabolic rate, are functionally linked and so they are constrained to co-evolve. These characters may constitute a case of the correlated progression concept (Kemp, 2007), the phylogeny being an explanatory (but not a causal) factor. On the other hand, the thickness of the outer layer of avascular bone tissue is significantly higher in lepidosaurs than in birds clearly showing a phylogenetic pattern which may be explained by different metabolic requirements of osteocytes in these clades. Future work on the effect of osteocyte size and density on the variation of both the thickness of the outer layer of avascular bone tissue and the bone vascular density in a more comprehensive sample of diapsids may allow additional tests of our hypotheses.

ACKNOWLEDGEMENTS

We thank very much reviewers Koen Stein and Michael D'Emic and associate editor Alexandra Houssaye for interesting suggestions that greatly improved the quality of the manuscript. This work was supported by the Spanish Gouvernement (grant CGL2011-23919 to JC), the Centre National de la Recherche Scientifique and the Université Pierre et Marie

Curie (operating grant of UMR 7193 to JC, JB, AQ and LL) and by the Centre National de la Recherche Scientifique and the Muséum National d'Histoire Naturelle (operating grant of UMR 7207 to VdB).

AUTHOR CONTRIBUTION

JC and VdB conceived research. JC and LL performed statistical analyses. JC wrote the paper. JB quantified histological data in birds and VdB in lepidosaurs. AQ performed the cytological study.

REFERENCES

Amprino R. 1947. La structure du tissue osseux envisagée comme l'expression de différences dans la vitesse de l'accroissement. *Arch. Biol.* **58:** 315-330.

Ast JC. 2001. Mitochondrial DNA evidence and evolution in Varanoidea (Squamata). *Cladistics* **17:** 211-226.

Barker FK, Barrowclough GF, Groth JG. 2002. A phylogenetic hypothesis for passerine birds: taxonomic and biogeographic implications of an analysis of nuclear DNA sequence data. *Proceedings of the Royal Society of London B* **269:** 295-308.

Bonewald LF. 2011. The amazing osteocyte. *Journal of Bone Mineral Research.* **26**:229–238.

Brookes M. 1971. *The blood supply of bone*. Butterworths and Co, London. 338 p.

Buffrénil V de, Houssaye A, Böhme W. 2008. Bone vascular supply in Monitor lizards (Squamata: Varanidae): influence of size, growth and phylogeny. *Journal of Morphology* **269:** 533-543.

Conrad JL. 2008. Phylogeny and systematics of Squamata (Reptilia) based on morphology. *Bulletin of the American Museum of Natural History* **310:** 1-182.

Cubo J, Ponton F, Laurin M, Margerie E de, Castanet J. 2005. Phylogenetic signal in bone microstructure of sauropsids. *Systematic Biology* **54:** 562-574.

Currey JD. 2002. *Bones* 2nd edition. Princeton University press: New Jersey, USA

Francillon-Vieillot H, deBuffrénil V, Castanet J, Géraudie J, Meunier FJ, Sire JY, Zylberberg L, de Ricqlès, A. 1990. Microstructure and mineralization of vertebrate skeletal tissues. In: Carter JG, editor. *Skeletal biomineralization: patterns, processes and evolutionary trends*, p. 471–530 [New York].

Grafen A. **1989**. The Phylogenetic Regression. *Philosophical Transactions of the Royal Society of London. Series B, Biological Sciences* **326**: 119–157.

Harvey PH, Pagel MD. 1991. *The comparative method in evolutionary biology.* Oxford: Oxfor University Press.

Hulbert AJ, Pamplona R, Buffenstein R, Buttemer WA. 2007. Life and death: metabolic rate, membrane composition and life span of animals. *Physiological Reviews* **87**: 1175-1213.

Kemp TS. 2007. The concept of correlated progression as the basis of a model for the evolutionary origin of major new taxa. *Proceedings of the Royal Society B: Biological Sciences* **274**: 1667–1673.

Kennedy OD, Schaffler MB. **2012**.The roles of osteocyte signaling in bone. *Journal of American Academy of Orthopaedic Surgeons*. **20**: 670–671.

Kerschnitzki M, Wagermaier W, Roschger P, Seto J, Shahar R, Duda GN, Mundlos S, Fratzl P. 2011. The organization of the osteocyte network mirrors the extracellular matrix orientation in bone. *Journal of Structural Biology*. **173** : 303-311.

Livezey BC, Zusi RL. 2007. Higher-order phylogeny of modern birds (Theropoda, Aves: Neornithes) based on comparative anatomy. II. Analysis and discussion. *Zoological Journal of the Linnean Society* **149:** 1-95.

Maddison WP. 1991. Squared-change parsimony reconstructions of ancestral states for continuous-valued characters on a phylogenetic tree. *Systematic Zoology* **40:** 304–314.

Maddison WP, Maddison DR. 2011. *Mesquite: A modular system for evolutionary analysis. Version 2.75.* Available at http://mesquiteproject.org

Midford P, Garland TJ, Maddison WP. 2011. *PDAP Package for Mesquite. Version 1.16*.

Available at http://mesquiteproject.org/pdap_mesquite/index.html

Mishra S. 2009. Biomechanical aspects of bone microstructures in vertebrates: potential approach to palaeontological investigations. *Journal of Biosciences* **34:** 799-809.

Orme D, Freckleton R, Thomas G, Petzoldt T, Fritz S, Isaac N, Pearse W. **2012**. The caper package: comparative analysis of phylogenetics and evolution in R. R package version 0.5.2

Ponton F, Elzanowski A, Castanet J, Chinsamy A, Margerie E de, Ricqlès A de, Cubo J. 2004. Variation of the outer circumferential layer in the limb bones of birds. *Acta Ornithologica* **39:** 137-140.

Pyron RA. 2010. A likelihood method for assessing molecular divergence time estimates and the placement of fossil calibrations. *Systematic Biology* **59**: 185-194.

Revell LJ. **2010**. Phylogenetic signal and linear regression on species data. *Methods in Ecology and Evolution* **1**: 319–329.

Simpson AHRW. 1985. The blood supply of the periosteum. *Journal of Anatomy* **140:** 697-704.

Schmidt-Nielsen K. 1997. *Animal physiology,* 5th edn. Cambridge: Cambridge University Press.

Schneider CA, Rasband WS, Eliceiri KW. 2012. NIH image to ImageJ: 25 years of image analysis. *Nature Methods* **9**: 671-675.

White CR, Phillips NF, Seymour RS. (2006). The scaling and temperature dependance of vertebrate metabolism. *Biology Letters* **2**: 125-127.

FIGURE LEGENDS

FIGURE 1. Fraction of a diaphyseal femoral transverse section of *Corvus corone* (Aves, Neognathae) showing the histological features quantified in this study. A. Histological section. B. Gray: bone cortex; black: vascular cavities. C. Gray: bone cortex minus the outer avascular layer; black: outer avascular layer.

FIGURE 2. Phylogenetic relationships among the sample of birds used in this study. Higher order relationships were taken from Livezey & Zusi (2007). Relationships among passeriforms were compiled from Barker *et al.* (2002). Branch lengths were taken from Pyron (2010).

FIGURE 3. Phylogenetic relationships among the sample of lepidosaurs used in this study. Higher order relationships and branch lengths were taken from Conrad (2008). Relationships among *Varanus* species were compiled from Ast (2001).

FIGURE 4. Femoral semi-thin (A - D) and ultra-thin (E) mid-shaft cross sections of *Anas*

platyrhynchos (A, B, E) and *Varanus exanthematicus* (C-D). A, In the periosteum (P), an osteoblast (Ob) is in close contact with a blood vessel (Bv). Osteocytes (Oc) are numerous in the periosteal bone (PB) and a rich canaliculi network is present. B, Canaliculi (Ca) are clearly directed towards the blood vessel located in the periosteal bone. C, Long canaliculi communicate with the periosteum where a blood vessel is visible. D, Osteocytes surrounding a blood vessel containing an erythrocyte (E). A rich canaliculi network is observed. E, Transmission electron microscopy micrograph showing a tight contact (black arrows) between the body cell of an osteocyte and the wall of a blood vessel where an erythrocyte is visible. The osteocyte shows long processes in the canaliculi throughout the bone matrix.

FIGURE 5. PGLS regression of the log thickness of the outer layer of avascular bone tissue with log bone radius in birds (R^2: 0.041; *p*-value: 0.146).

FIGURE 6. PGLS regression of the log bone vascular density with log snout-vent maximal length in *Varanus* (R^2: 0.210; *p*-value: 0.024).

Table 1. Dataset corresponding to the sample of birds

Species	Bone cross sectional area, mm^2	Thickness outer layer avascular bone, mm	Bone vascular density, $1/mm^2$	Bone vascular area / Bone cortical area
Accipiter nisus	15.148	0.092	83.544	0.020
Alcedo atthis	1.916	0.079	69.069	0.006
Alectura lathami	80.828	0.043	89.291	0.080
Apus apus	1.450	0.102	0.000	0.000
Asio flammeus	13.703	0.05	81.832	0.022
Asio otus	9.038	0.099	124.238	0.028
Bubulcus ibis	17.500	0.051	149.603	0.035
Buteo buteo	31.349	0.102	71.583	0.026
Chroicocephalus ridibundus	16.243	0.057	79.141	0.023
Columba palumbus	12.000	0.055	110.776	0.031
Corvus corone	13.335	0.092	65.909	0.023
Dendrocopos major	4.095	0.122	33.247	0.004
Emberiza citrinella	1.275	0.114	0.000	0.000
Erithacus rubecula	1.112	0.116	0.000	0.000
Falco tinnunculus	8.379	0.089	98.127	0.030
Fulica atra	16.388	0.094	79.106	0.022
Megapodius nicobariensis	25.668	0.121	69.318	0.036
Parus caeruleus	0.859	0.086	0.000	0.000
Parus major	1.626	0.092	0.000	0.000
Pica pica	6.733	0.09	70.151	0.025
Picus viridis	6.274	0.067	48.317	0.008
Podiceps cristatus	16.620	0.033	122.169	0.065
Scolopax rusticola	12.755	0.102	81.699	0.015
Streptopelia decaocto	7.126	0.044	82.321	0.016
Strix aluco	21.400	0.069	93.447	0.02
Sturnus vulgaris	4.954	0.088	21.465	0.003

Sylvia atricapilla	1.080	0.049	0.000	0.000
Tringa hypoleucos	2.210	0.046	82.636	0.017
Troglodytes troglodytes	0.808	0.096	0.000	0.000
Turdus philomelos	4.377	0.079	26.600	0.004

Table 2. Dataset corresponding to the sample of lepidosaurs

Species	Bone cross sectional area, mm^2	Thickness outer layer avascular bone, mm	Bone vascular density, $1/mm^2$	Bone vascular area / Bone cortical area
Agama atra	2.490	0.422	0.000	0.000
Agama bibroni	2.320	0.380	0.000	0.000
Amblyrhynchus cristatus	29.158	1.455	0.000	0.000
Ameiva ameiva	2.050	0.265	0.000	0.000
Ameiva bifrontala	2.490	0.350	0.000	0.000
Barisia imbricata	0.561	0.231	0.000	0.000
Callopistes maculatus	3.750	0.480	0.000	0.000
Cnemidophorus deppei	0.480	0.120	0.000	0.000
Cnemidophorus lemniscatus	1.040	0.230	0.000	0.000
Coleonyx elegans	0.208	0.059	0.000	0.000
Corucia zebrata	10.290	0.000	0.130	0.007
Crocodilurus lacertinus	5.030	0.760	0.000	0.000
Ctenosaura pectinata	23.022	0.702	0.000	0.000
Dipsosaurus dorsalis	1.609	0.242	0.000	0.000
Dracaena guianensis	17.950	0.000	6.760	0.369
Gallotia atlantica	0.875	0.221	0.000	0.000
Gallotia galloti	0.919	0.279	0.000	0.000
Gallotia goliath	18.390	0.940	0.000	0.000
Gerrhonotus viridiflavus	2.730	0.363	0.000	0.000
Heloderma horridum	13.219	1.018	0.000	0.000

Iguana iguana	17.843	0.800	0.000	0.000
Lacerta lepida	5.970	0.770	0.000	0.000
Lacerta viridis	1.509	0.391	0.000	0.000
Podarcis boccagei	0.319	0.188	0.000	0.000
Podarcis muralis	0.360	0.195	0.000	0.000
Pogona vitticeps	5.013	0.507	0.000	0.000
Sauromalus obesus	5.655	0.495	0.000	0.000
Sceloporus gadoviae	0.446	0.138	0.000	0.000
Sceloporus horridus	0.511	0.104	0.000	0.000
Sphenodon punctatus	10.281	1.057	0.055	0.003
Tupinambis rufescens	13.135	0.000	29.915	2.855
Tupinambis teguixin	15.327	0.000	11.177	0.188
Uromastyx aegyptiacus	10.791	0.655	0.000	0.000
Urosaurus bicarinatus	0.326	0.129	0.000	0.000
Varanus bengalensis	18.290	0.000	13.850	0.650
Varanus caudolineatus	0.640	0.220	0.000	0.000
Varanus doreanus	31.407	0.000	11.163	0.387
Varanus exanthematicus	24.233	0.000	17.953	2.410
Varanus flavescens	16.465	0.000	7.155	0.130
Varanus gilleni	1.415	0.372	0.000	0.000
Varanus glebopalma	7.115	0.475	0.000	0.000
Varanus gouldii	13.535	0.000	7.410	0.530
Varanus griseus	10.220	0.000	33.330	0.620
Varanus indicus	14.590	0.000	5.790	0.060
Varanus macrei	6.483	0.680	0.000	0.000
Varanus mertensi	25.510	0.000	11.050	0.250
Varanus niloticus	34.542	0.000	28.424	2.111
Varanus ornatus	18.255	0.000	12.785	0.385
Varanus prasinus	6.637	0.610	0.000	0.000
Varanus rudicollis	18.973	0.000	43.803	1.595

Varanus salvator	47.417	0.000	13.043	1.150
Varanus timorensis	8.040	0.000	0.300	0.000
Varanus varius	78.020	0.000	3.710	0.390
Varanus yuwonoi	17.390	0.000	14.565	0.965

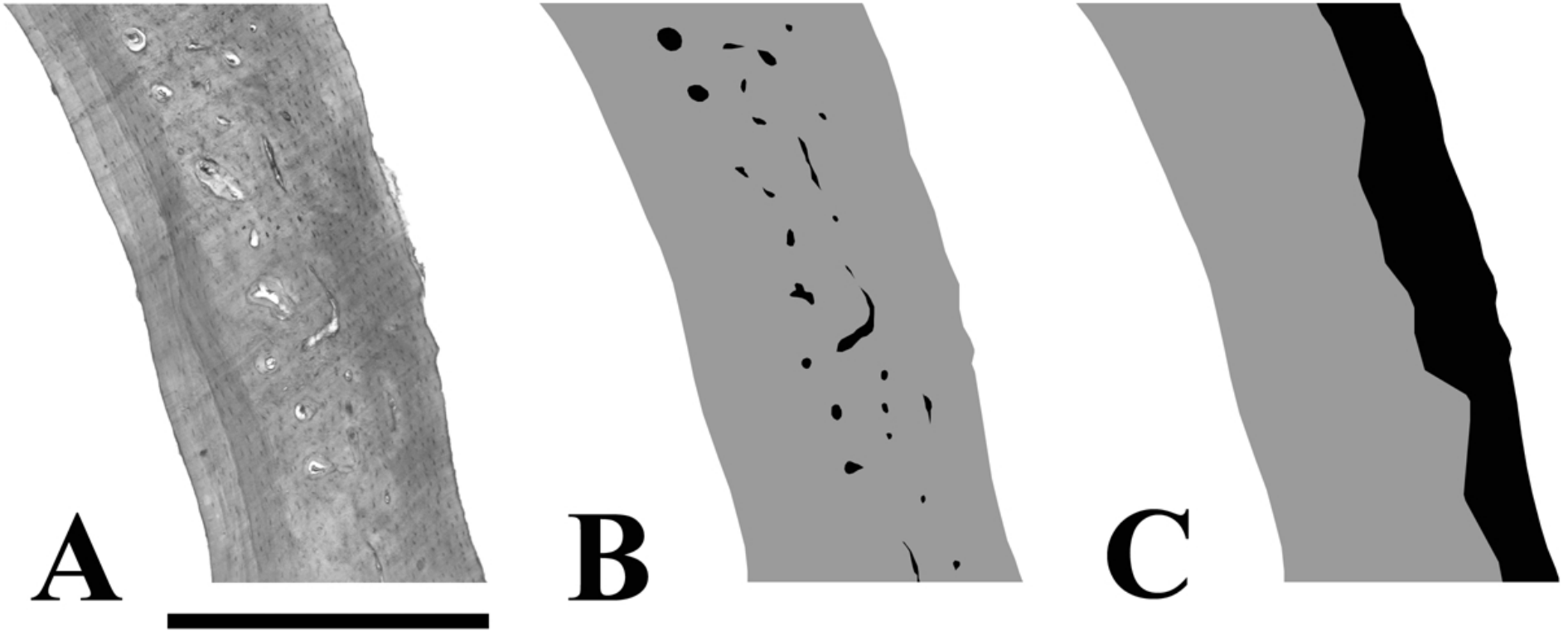
A
B
C

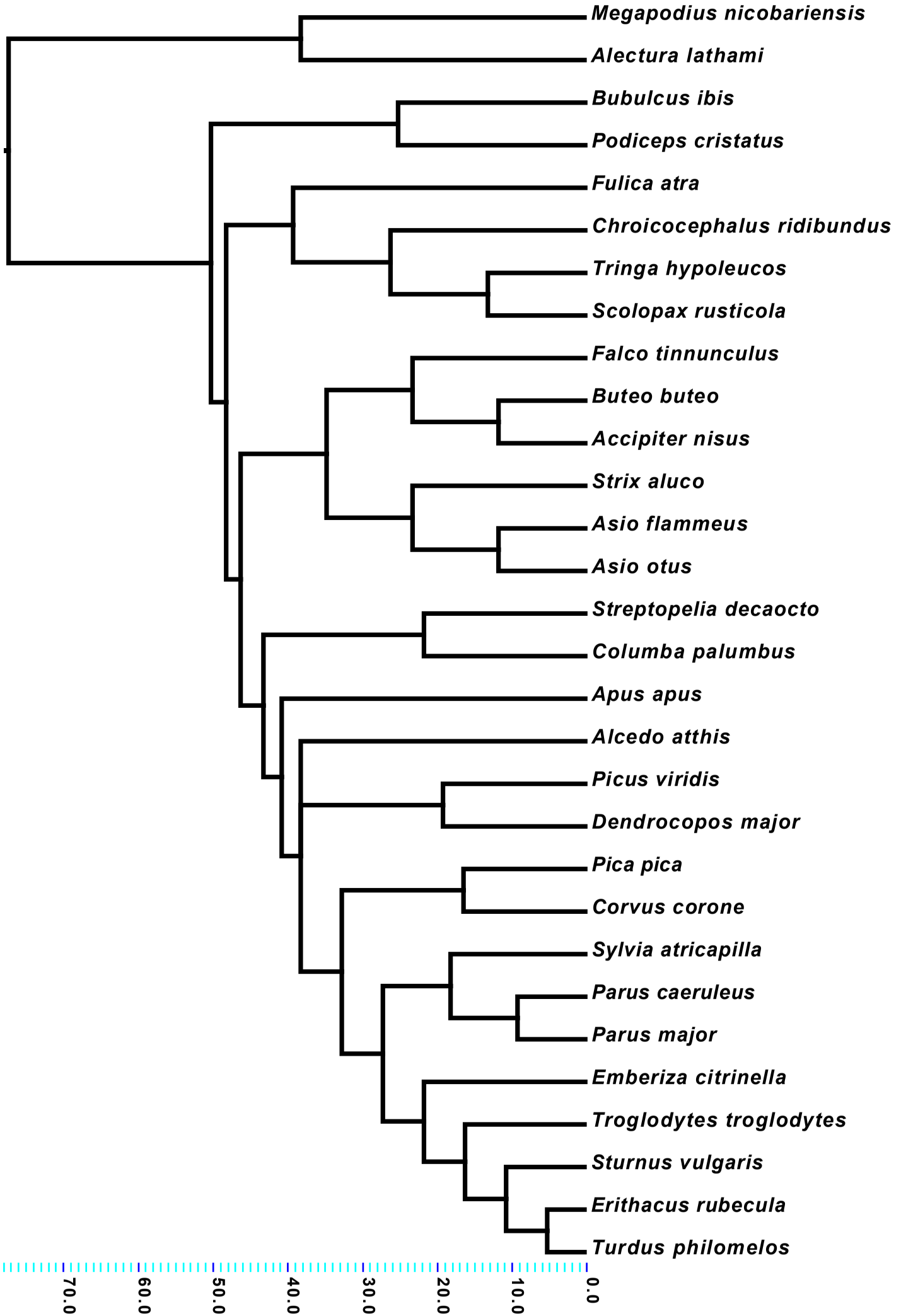
Megapodius nicobariensis
Alectura lathami
Bubulcus ibis
Podiceps cristatus
Fulica atra
Chroicocephalus ridibundus
Tringa hypoleucos
Scolopax rusticola
Falco tinnunculus
Buteo buteo
Accipiter nisus
Strix aluco
Asio flammeus
Asio otus
Streptopelia decaocto
Columba palumbus
Apus apus
Alcedo atthis
Picus viridis
Dendrocopos major
Pica pica
Corvus corone
Sylvia atricapilla
Parus caeruleus
Parus major
Emberiza citrinella
Troglodytes troglodytes
Sturnus vulgaris
Erithacus rubecula
Turdus philomelos
70.0
60.0
50.0
40.0
30.0
20.0
10.0
0.0

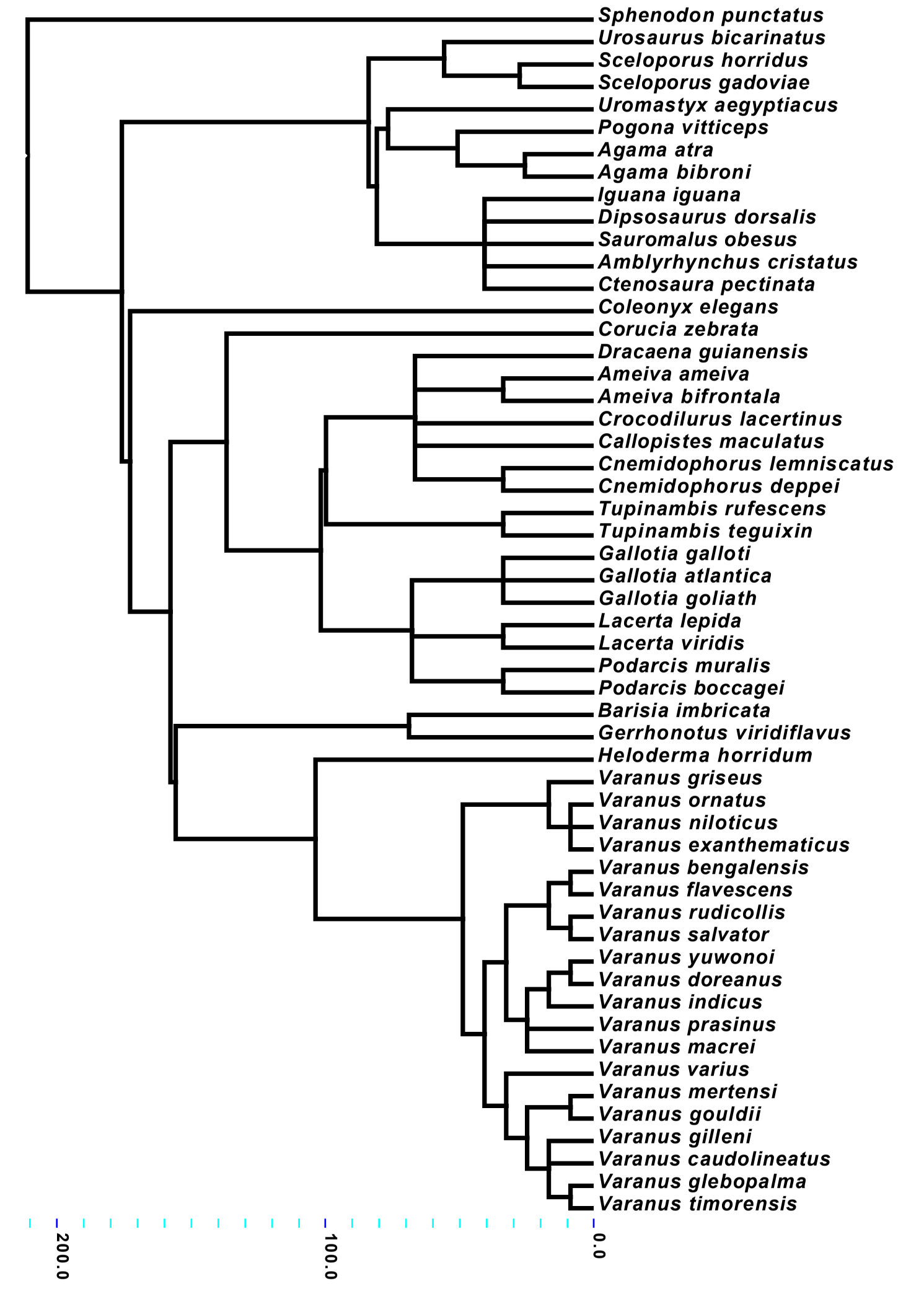
Sphenodon punctatus
Urosaurus bicarinatus
Sceloporus horridus
Sceloporus gadoviae
Uromastyx aegyptiacus
Pogona vitticeps
Agama atra
Agama bibroni
Iguana iguana
Dipsosaurus dorsalis
Sauromalus obesus
Amblyrhynchus cristatus
Ctenosaura pectinata
Coleonyx elegans
Corucia zebrata
Dracaena guianensis
Ameiva ameiva
Ameiva bifrontala
Crocodilurus lacertinus
Callopistes maculatus
Cnemidophorus lemniscatus
Cnemidophorus deppei
Tupinambis rufescens
Tupinambis teguixin
Gallotia galloti
Gallotia atlantica
Gallotia goliath
Lacerta lepida
Lacerta viridis
Podarcis muralis
Podarcis boccagei
Barisia imbricata
Gerrhonotus viridiflavus
Heloderma horridum
Varanus griseus
Varanus ornatus
Varanus niloticus
Varanus exanthematicus
Varanus bengalensis
Varanus flavescens
Varanus rudicollis
Varanus salvator
Varanus yuwonoi
Varanus doreanus
Varanus indicus
Varanus prasinus
Varanus macrei
Varanus varius
Varanus mertensi
Varanus gouldii
Varanus gilleni
Varanus caudolineatus
Varanus glebopalma
Varanus timorensis
200.0
100.0
0.0

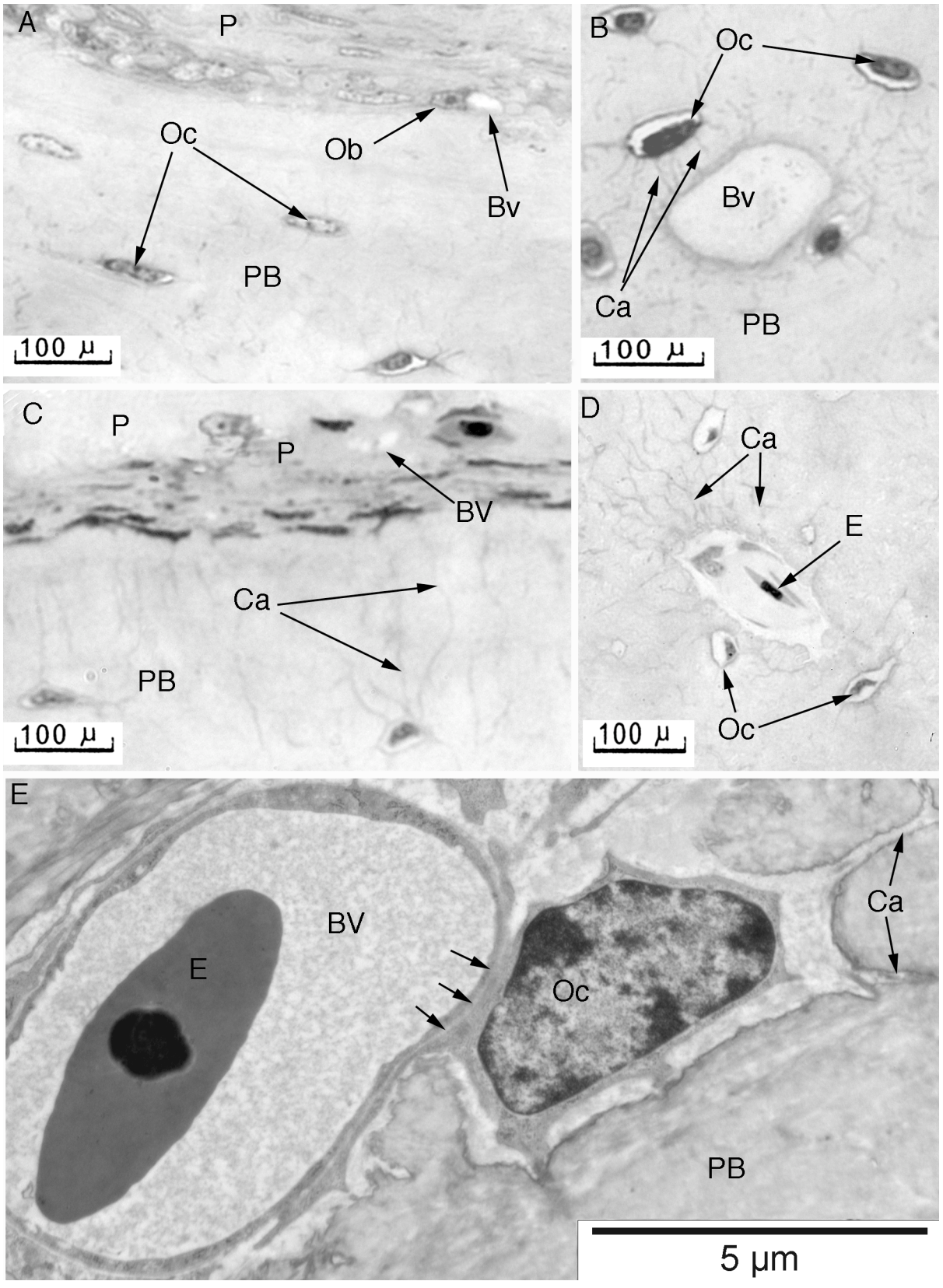
A
P
Oc
Ob
Bv
PB
100 µ
B
Oc
Bv
Ca
PB
100 µ
C
P
P
BV
Ca
PB
100 µ
D
Ca
E
Oc
100 µ
E
BV
E
Oc
Ca
PB
5 µm

Log thickness outer layer avasc. bone
−0.9
−1.1
−1.3
−1.5
−0.2
0.0
0.2
0.4
0.6
Log bone radius


Bone vascular density
0
10
30
2.2
2.4
2.6
2.8
3.0
Log snout-vent length